BIOMOLECULES & THERAPEUTICS

Original Article
Biomol Ther 33(3), 429-437 (2025)

MLKL Inhibitor Reduces Oxidative Stress, Inflammation, and Dopaminergic Neuronal Cell Death in MPTP-Induced Parkinson's Disease Mouse Model

Do-Yeon Kim, Yea-Hyun Leem and Hee-Sun Kim*

Department of Molecular Medicine and Inflammation-Cancer Microenvironment Research Center, School of Medicine, Ewha Womans University, Seoul 07804, Republic of Korea

Abstract

Parkinson's disease (PD) is a movement disorder characterized by the progressive loss of dopaminergic neurons in the substantia nigra (SN). Recent studies have shown that necroptosis is involved in the development of inflammatory and neurodegenerative diseases. Receptor-interacting protein kinase (RIPK)1, RIPK3, and mixed lineage kinase domain-like protein (MLKL) play key roles in necroptosis, with MLKL being the final executor of necroptosis. Necrosulfonamide (NSA) is a specific inhibitor of MLKL, and its therapeutic effects in various inflammatory and neurological disorders have been previously reported. However, its role in PD has not yet been clearly demonstrated. In this study, we examined the effects of NSA in a 1-methyl-4-phenyl-1,2,3,6-tetrahydropyridine (MPTP)-induced mouse model of PD. NSA reduced dopaminergic cell death and restored the expression of neurotrophic factors, such as BDNF, GDNF, and PGC-1α, in the SN region of MPTP mice. In addition, NSA inhibited microglial/astrocyte activation and the expression of proinflammatory markers, such as iNOS, TNF-α, IL-1β, and IL-6. NSA also reduced oxidative stress markers, such as 8-OHdG and 4-HNE, while enhancing Nrf2-driven antioxidant enzymes, including HO-1, catalase, MnSOD, GCLC, and GCLM. We found that NSA inhibited MLKL phosphorylation in dopaminergic neurons and microglia, which may have reduced neuronal cell death and inflammation. Therefore, NSA-mediated suppression of dopaminergic neuronal cell death, inflammation, and oxidative stress may have therapeutic potential in PD.

Key Words: Parkinson's disease, MLKL, Necrosulfonamide, Neuroinflammation, Oxidative stress, Nrf2 signaling

INTRODUCTION

Parkinson's disease (PD) ranks as the second most prevalent neurodegenerative disorder globally, following dementia, and affects an estimated 7 to 10 million individuals worldwide (Furgiuele *et al*., 2023). From a pathological perspective, PD is marked by the progressive degeneration of dopaminergic neurons in the substantia nigra pars compacta (SNpc), a subsequent reduction of dopamine in the striatum, accumulation of alpha-synuclein aggregates known as Lewy bodies, and neuroinflammation (Poewe *et al*., 2017; Calabresi *et al*., 2023; Ye *et al*., 2023). Clinically, PD is characterized by motor symptoms such as tremors at rest, stiffness, slowness of movement (bradykinesia), and impaired postural balance (Antonini *et al*., 2023; Stocchi *et al*., 2024). Increasing evidence indicates that neuroinflammation and oxidative stress are key contributors to the progression of PD (Taylor *et al*., 2013; Chang and Chen, 2020; Henrich *et al*., 2023). Factors such as aging, infections, genetic alterations, and exposure to environmental neurotoxins can activate microglia and astrocytes, triggering the release of inflammatory cytokines and reactive oxygen species (ROS). This proinflammatory and oxidative environment exerts harmful effects on healthy neurons, ultimately leading to the degeneration of dopaminergic neurons (Taylor *et al*., 2013; Rai and Singh, 2020). Therefore, targeting neuroinflammation and oxidative stress has emerged as a promising therapeutic strategy for the treatment of PD.

Recent studies have reported that necroptosis, a programmed necrosis, is implicated in various neurodegenerative diseases, including PD, Alzheimer's disease, amyotrophic lateral sclerosis, and multiple sclerosis (Ofengeim *et al*., 2015; Ito *et al*., 2016; Caccamo *et al*., 2017; Lin *et al*., 2020). Under necroptotic conditions, activated receptor-interacting protein kinase (RIPK)1 phosphorylates RIPK3, which subsequently

Open Access **https://doi.org/10.4062/biomolther.2025.049**

Received Mar 18, 2025 **Revised** Apr 1, 2025 **Accepted** Apr 4, 2025
Published Online Apr 15, 2025

***Corresponding Author**
E-mail: hskimp@ewha.ac.kr
Tel: +82-2-6986-6270, Fax: +82-2-6986-7014

phosphorylates mixed lineage kinase domain-like protein (MLKL), forming a necrosome complex. p-MLKL then oligomerizes and translocates to the plasma membrane, causing its rupture (Molnár *et al*., 2019; Tang and Zhuang, 2024). Necroptotic cells release damage-associated molecular patterns (DAMPs) that trigger inflammation in surrounding cells (Kearney and Martin, 2017). As a key effector of necroptosis, MLKL plays a pivotal role in necroptotic cell death and the subsequent inflammatory response, making it a compelling target for drug development (Zhao *et al*., 2012; Zhang *et al*., 2022).

Necrosulfonamide (NSA) is a selective inhibitor of MLKL that blocks necroptosis by targeting the N-terminal domain (Liu *et al*., 2017; Tang and Zhuang, 2024). Recent research has demonstrated the therapeutic potential of NSA in animals with inflammatory and neurological disorders. NSA ameliorates colitis, hyperalgesia, and sepsis-associated encephalopathy by inhibiting inflammation (Rathkey *et al*., 2018; Ozgen *et al*., 2023; Fu *et al*., 2024). Moreover, NSA exerts neuroprotective effects in animal models of Alzheimer's disease, intracerebral hemorrhage, cerebral ischemia, and spinal cord injury (Jiao *et al*., 2020; Motawi *et al*., 2020; Zhang *et al*., 2022; Zhou *et al*., 2023). A recent study by our group reported that NSA inhibited α-synuclein oligomerization and necroptosis in a subacute 1-methyl-4-phenyl-1,2,3,6-tetrahydropyridine (MPTP) mouse model of PD (Leem *et al*., 2023). However, the effects and molecular mechanisms of NSA on neuroinflammation and oxidative stress remain unclear. Furthermore, the effect of NSA on acute MPTP mouse models has not been reported. Therefore, this study aimed to explore the therapeutic potential of NSA and its underlying molecular mechanisms, focusing on oxidative stress and neuroinflammation in mice subjected to acute MPTP treatment.

MATERIALS AND METHODS

Reagents and antibodies

NSA was obtained from Merck Millipore (Billerica, MA, USA). MPTP was purchased from the Tokyo Chemical Industry Co. (Tokyo, Japan). The primary antibodies used were as follows: anti-TH, anti-p-MLKL, anti-MLKL, and anti-β-actin antibodies from Cell Signaling Technology (Danvers, MA, USA); anti-IL-6, anti-TNF-α, anti-Nrf2, and anti-catalase antibodies from Santa Cruz Biotechnology (Dallas, TX, USA); anti-GCLC and anti-IL-1β from Mybiosource (San Diego, CA, USA); anti-iNOS from BD Bioscience (San Jose, CA, USA); anti-BDNF from Sigma-Aldrich (St Louis, MO, USA); anti-GDNF from Abcam (Waltham, MA, USA); anti-PGC-1α from Merck Millipore; anti-GCLM from GeneTex (Irvine, CA, USA); anti-HO-1 and anti-MnSOD from Enzo Life Sciences (Farmingdale, NY, USA); anti-4-HNE from Alpha diagnostic Intl Inc. (San Antonio, TX, USA); and anti-OX-42 from Bio-Rad (Hercules, CA, USA).

Animals

Male C57BL/6 mice (24-25 g, 9-10 weeks old) were obtained from Orient Bio, Inc. (Seongnam, Korea). The animals were maintained at a constant temperature of 21°C under a 12-hour light/dark cycle, with unrestricted access to food and water. All efforts were undertaken to minimize animal discomfort. Experimental procedures were conducted in accordance with the guidelines of the National Institutes of Health and Ewha Womans University for the care and use of laboratory animals, and were approved by the Institutional Animal Care and Use Committee of the Ewha Womans University Medical School (EWHA MEDIACUC 21-012).

Drug administration

To study the MPTP-induced PD mouse model, C57BL/6 mice were randomly divided into six groups (control, MPTP, MPTP+NSA 1 mg/kg, MPTP+NSA 5 mg/kg, NSA 1 mg/kg, and NSA 5 mg/kg; n=8-10 per group). NSA was dissolved in the vehicle (1% DMSO in normal saline) and administered intraperitoneally (i.p.) for 3 days. One day after the final NSA treatment, mice were injected with MPTP (20 mg/kg, i.p.) four times at 2 h intervals and were sacrificed 7 days after MPTP injection (Jackson-Lewis and Przedborski, 2007).

Brain tissue preparation

For histological examinations, mice were anesthetized with sodium pentobarbital (80 mg/kg; Hanlim Pharm Co. Ltd., Seoul, Korea) and perfused transcardially with 0.9% saline, followed by 4% paraformaldehyde to fix the tissues. The brains were subsequently extracted and immersed in 30% sucrose at 4°C for cryoprotection. For biochemical studies, mice underwent transcardial perfusion with 0.9% saline only. Coronal brain sections (40 μm thick) were prepared using a cryotome (CM 1860; Leica, Wetzlar, Germany) for histological analysis.

Immunohistochemistry and immunofluorescence staining

For immunohistochemical (IHC) staining, tissue sections were first treated to suppress endogenous peroxidase activity and to block non-specific antibody binding. Sections were incubated overnight at 4°C with the primary antibody diluted in 4% BSA blocking buffer. Afterward, they were incubated for 1 h at room temperature with biotinylated secondary antibodies, followed by 1.5 h in an avidin-biotin-HRP complex solution (Vector Laboratories, Burlingame, CA, USA). Subsequently, the peroxidase reaction was performed using diaminobenzidine tetrahydrochloride solution (Vector Laboratories). For co-immunofluorescence (IF) staining, sections were incubated with primary antibody overnight at 4°C, followed by incubation with fluorophore-conjugated secondary antibodies (Alexa Fluor 488 and 594). The slides were then covered with the VECTASHIELD antifade mounting medium (Vector Laboratories). Digital images of IHC and IF staining were captured using a Leica DM750 microscope and quantified using ImageJ software (version 1.37; NIH, Bethesda, MD, USA).

Preparation of protein extracts and western blot analysis

Brain tissues from the substantia nigra (SN) were homogenized in lysis buffer supplemented with a protease inhibitor cocktail (Complete Mini, Roche, Mannheim, Germany). The lysates were vigorously vortexed and incubated at 4°C for 30 min. Subsequently, samples were centrifuged at 20,000×g for 30 min, and the resulting supernatants were collected. Protein samples (30-70 μg) were resolved by SDS-PAGE, transferred to nitrocellulose membranes, and incubated with primary antibodies prepared according to the manufacturer's recommendations. Following thorough washing with TBST, membranes were incubated with HRP-conjugated secondary antibodies (Bio-Rad; 1:2000 in 5% skim milk). Protein bands were visualized using an enhanced chemiluminescence detection kit (Thermo Fisher Scientific, Waltham, MA, USA). Band intensities were quantified and normalized to β-actin using ImageJ

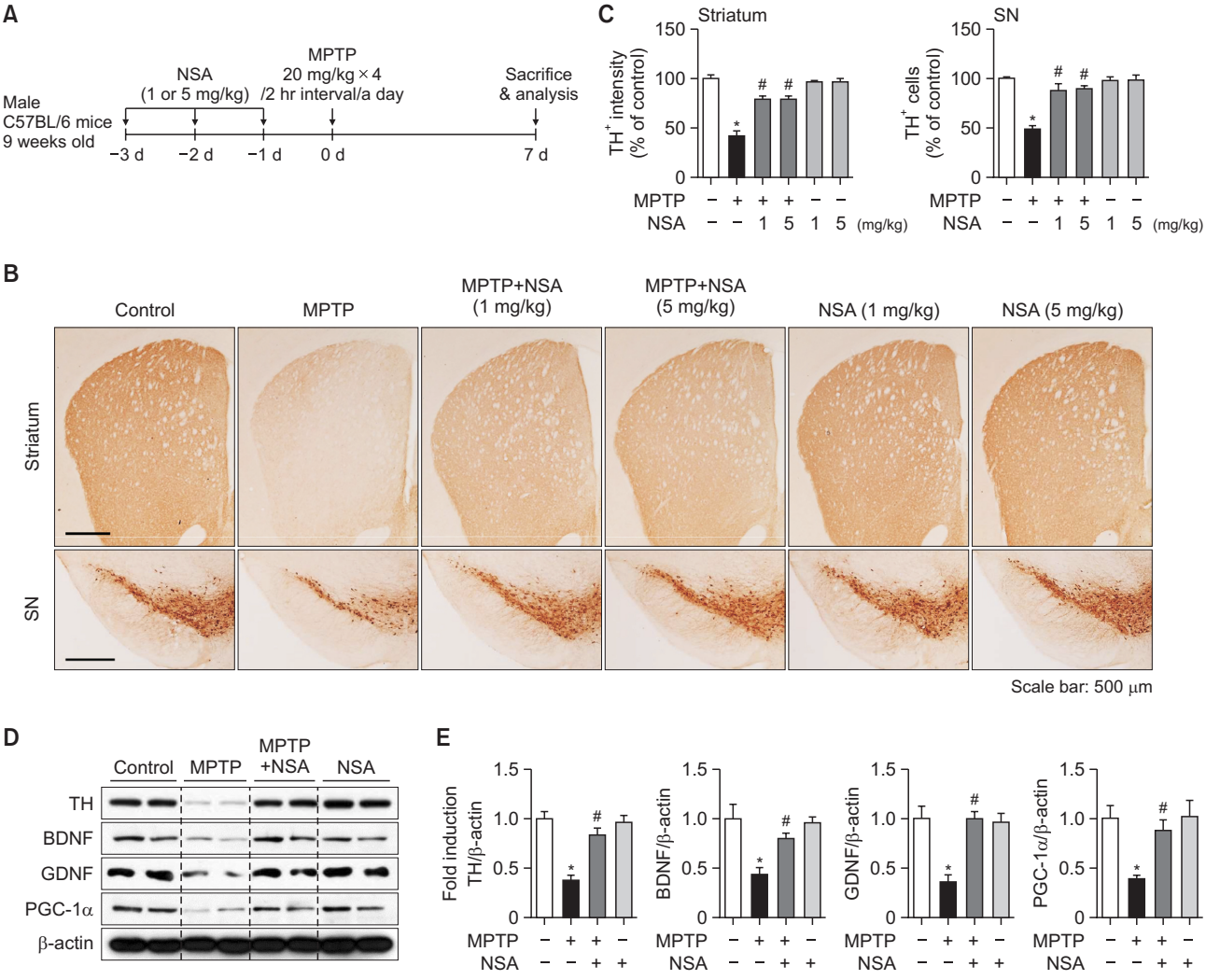

Fig. 1. Effects of necrosulfonamide (NSA) on dopaminergic neuronal cell death in the brains of MPTP-injected mice. (A) Schematic representation of experimental procedures. NSA (1 or 5 mg/kg, i.p.) or vehicle was administered daily for 3 days before MPTP treatment (20 mg/kg, four injections at 2-hour intervals). (B) Representative immunostained images of TH-positive neurons in the striatum and SN (n=4-5 per group). (C) Quantitative analysis was conducted by assessing the optical density of TH-positive fibers in the striatum and counting TH-positive cells in the SN. (D) Western blot data showing the effect of NSA on the expression of TH, BDNF, GDNF, and PGC-1α in the SN (n=4 per group). (E) Quantification of western blot data. Data are shown as the mean ± SEM. *p<0.05 vs. control group; $^{\#}p$<0.05 vs. MPTP group. MPTP, 1-methyl-4-phenyl-1,2,3,6-tetrahydropyridine; TH, tyrosine hydroxylase; BDNF, brain-derived neurotrophic factor; GDNF, glial cell-derived neurotrophic factor; PGC-1α, peroxisome proliferator-activated receptor-gamma coactivator-1 alpha.

software (version 1.37; NIH, Bethesda, MD, USA).

Statistical analysis

Statistical differences among experimental groups were evaluated using one-way analysis of variance (ANOVA), followed by post-hoc analysis with the least significant difference (LSD) test. All statistical analyses were conducted using SPSS software for Windows (version 18.0; SPSS Inc., Armonk, NY, USA). Data are expressed as mean ± standard error of the mean (SEM). Statistical significance was set at p<0.05.

RESULTS

NSA reduced dopaminergic cell death and restored neurotrophic factors in MPTP-treated mice

To examine the neuroprotective effects of NSA, mice were administered NSA for three days before being injected with MPTP. Seven days following MPTP administration, mice were sacrificed for subsequent histological and biochemical analyses (Fig. 1A). These findings revealed that NSA recovered striatal dopaminergic fibers, as evidenced by an increased optical density of TH$^+$ fibers in the striatum. Furthermore, NSA restored nigral dopaminergic cells, as evidenced by the increased number of nigral TH$^+$ cells in the brains of MPTP-injected mice (Fig. 1B, 1C). Subsequently, we examined the effect of NSA on the expression of TH and neurotrophic fac-

tors in the SN of MPTP mice. Western blot analysis showed that NSA restored the protein expression of TH, BDNF, GDNF, and PGC-1α, which were lowered by MPTP treatment (Fig. 1D, 1E).

NSA inhibited the activation of microglia and astrocytes, as well as the expression of proinflammatory markers in MPTP-treated mice

To investigate whether NSA inhibits glial cell activation, immunohistochemical staining was performed using antibodies against Iba-1 (a marker of microglial activation) and GFAP (a marker of astrocyte activation). The results showed that NSA

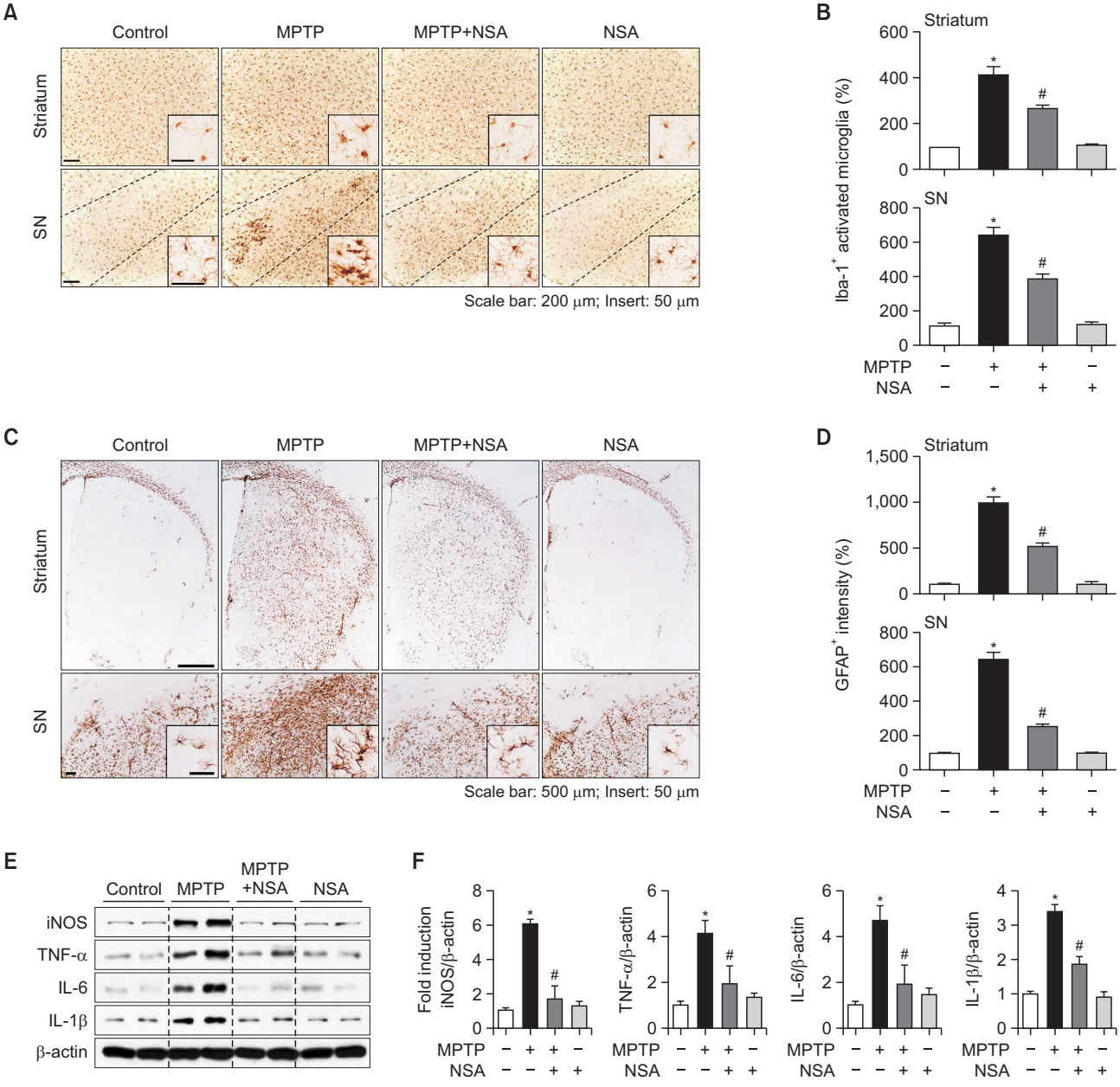

Fig. 2. Effects of NSA on microglia/astrocyte activation and the expression of pro-inflammatory markers in the brains of MPTP-injected mice. (A) Immunohistochemical staining for Iba-1 in the striatum and SN (dotted line: SNpc) (n=4-5 per group). (B) Quantification of the number of Iba-1-positive-activated microglia in the striatum and SN. (C) Immunohistochemical staining for GFAP in the striatum and SN (n=4-5 per group). (D) A histogram of the intensity of GFAP-positive cells in the striatum and SN. (E) Western blot data showing the effect of NSA on the expression of iNOS, TNF-α, IL-6, and IL-1β in the SN (n=4 per group). (F) Quantification of western blot data. Data are shown as the mean ± SEM. *p<0.05 vs. control group; $^{\#}p$<0.05 vs. MPTP group. Iba-1, ionized calcium-binding adapter molecule1; SNpc, substantia nigra pars compacta; GFAP, glial fibrillary acidic protein; iNOS, inducible nitric oxide synthase; TNF-α, tumor necrosis factor-α; IL-1β, interleukin-1β.

reduced the number of activated microglia in the striatum and SN of MPTP mice (Fig. 2A, 2B). NSA also reduced the number of reactive astrocytes in the striatum and SN (Fig. 2C, 2D). When we examined the effect of NSA on the protein expression of proinflammatory markers, NSA reduced the expression of iNOS, TNF-α, IL-1β, and IL-6 in the SN of MPTP mice (Fig. 2E, 2F). These findings demonstrate that NSA exerts anti-inflammatory effects in MPTP mice.

NSA decreased oxidative damage products while enhancing Nrf2-driven antioxidant enzymes in MPTP-treated mice

As oxidative stress plays an important role in PD development, we investigated the effect of NSA on oxidative damage in MPTP mice. 4-hydroxynonenal (4-HNE) is a lipid peroxidation product, and 8-hydroxy-2'-deoxyguanosine (8-OHdG) is a DNA damage marker. Co-IF staining showed that NSA

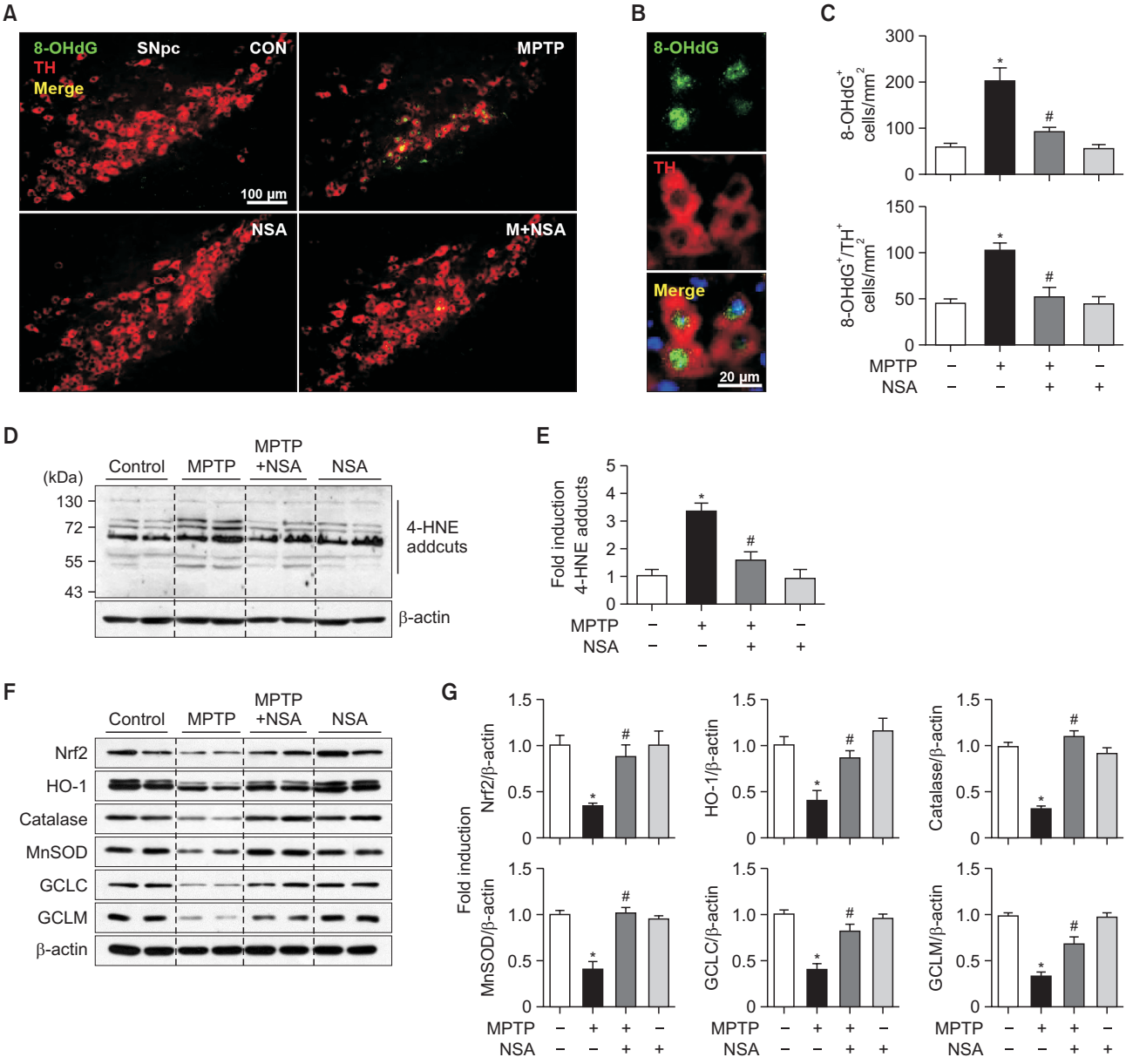

Fig. 3. Effects of NSA on oxidative stress markers in the brains of MPTP-injected mice. (A) Co-IF staining for 8-OHdG (a marker for oxidative damage of DNA, green) and TH (a marker of dopaminergic neurons, red) in the SNpc of MPTP-injected mice (n=4-5 per group). (B) High magnitude images (8-OHdG, green; TH, red; DAPI, blue). (C) Quantification of 8-OHdG-positive and 8-OHdG$^+$/TH$^+$ cells. (D) Western blot data showing the effect of NSA on the expression of 4-HNE in the SN (n=4 per group). (E) Quantification of western blot data. (F) Western blot data showing the effect of NSA on the expression of Nrf2, HO-1, catalase, MnSOD, GCLC, and GCLM in the SN (n=4 per group). (G) Quantification of western blot data. Data are shown as the mean ± SEM. *p<0.05 vs. control group; #p<0.05 vs. MPTP group. 8-OHdG, 8-hydroxy-2'-deoxyguanosine; 4-HNE, 4-hydroxynonenal; Nrf2, nuclear factor erythroid 2-related factor 2; HO-1, hemeoxygenase-1; MnSOD, manganese superoxide dismutase; GCLC, γ-glutamyl cysteine ligase-catalytic subunit; GCLM, γ-glutamyl cysteine ligase-modulator subunit.

reduced 8-OHdG production in TH$^+$ dopaminergic neurons in the SN of MPTP mice (Fig. 3A-3C). Furthermore, NSA decreased the formation of 4-HNE adducts induced by MPTP (Fig. 3D, 3E). To evaluate the antioxidant mechanism of NSA, we tested its effects on Nrf2-driven phase II antioxidant enzymes. Western blot analysis demonstrated that NSA restored the expression of Nrf2 and its downstream targets HO-1, catalase, MnSOD, GCLC, and GCLM, which were decreased by MPTP treatment (Fig. 3F, 3G). These results indicated that NSA exerts an antioxidant effect by modulating the Nrf2 signaling pathway in MPTP-treated mice.

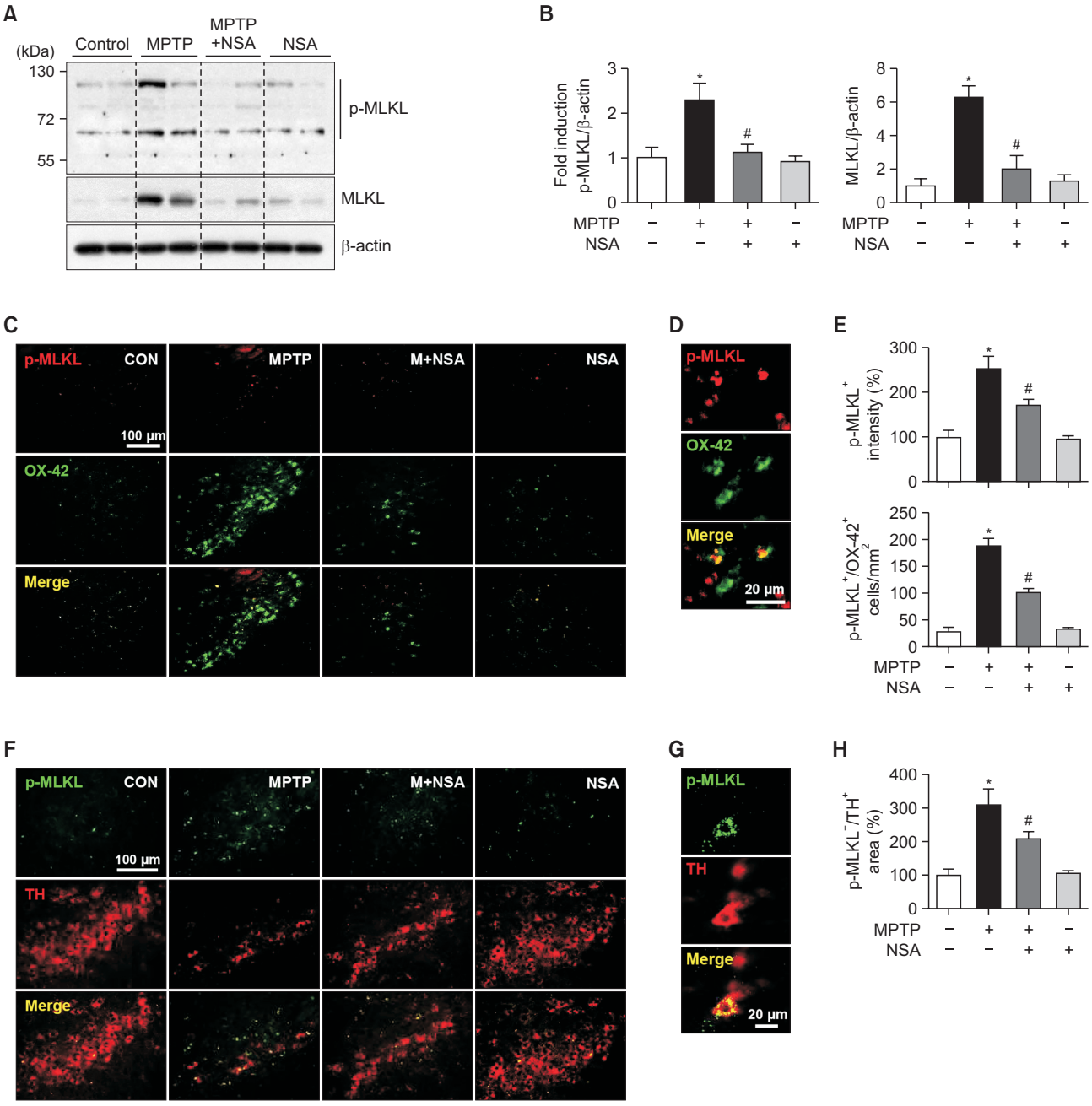

Fig. 4. Effects of NSA on phosphorylation and expression of MLKL in the brains of MPTP-injected mice. (A) Western blot data showing the effect of NSA on the expression of phospho- or total MLKL in the SN (n=4 per group). (B) Quantification of western blot data. (C) Co-IF staining for p-MLKL (hallmark of necroptosis, red) and OX-42 (marker for microglial cells, green) in the SN of MPTP-injected mice (n=4-5 per group). (D) High magnitude images and (E) quantification of p-MLKL-positive cells and p-MLKL$^+$/OX-42$^+$ cells. (F) Co-IF staining staining for p-MLKL (green) and TH (red) in the SN of MPTP-injected mice (n=4-5 per group). (G) High magnitude images and (H) quantification of p-MLKL$^+$/TH$^+$ cells. Data are shown as the mean ± SEM. *p<0.05 vs. control group; $^{\#}p$<0.05 vs. MPTP group. MLKL, mixed lineage kinase domain-like protein, SN, substantia nigra; Co-IF, co-immunofluorescence; TH, tyrosine hydroxylase.

NSA decreased MLKL phosphorylation in dopaminergic neurons and microglia in the SN of MPTP mice

To investigate whether necroptosis was involved in dopaminergic cell death and inflammation in our model system, we examined the effects of MPTP and/or NSA on MLKL phosphorylation and expression. Western blot analysis revealed that MPTP increased the phosphorylation and expression of MLKL in the SN of MPTP mice, which was reduced by NSA treatment (Fig. 4A, 4B). To determine the cell types expressing p-MLKL in MPTP mice, we performed co-IF labeling with antibodies against p-MLKL, OX-42 (a marker for microglia), GFAP (a marker for astrocyte), and TH (a marker for DA neurons). MPTP increased the number of p-MLKL$^+$/OX-42$^+$ and p-MLKL$^+$/TH$^+$ cells in the SN, which was blocked by NSA (Fig. 4C-4H). In contrast, p-MLKL$^+$/GFAP$^+$ cells were not observed, suggesting that astrocytic expression of p-MLKL was absent under these conditions (Supplementary Fig. 1). These findings indicate that NSA-mediated suppression of neuronal and microglial p-MLKL may exert neuroprotective and anti-inflammatory effects.

DISCUSSION

In this study, we demonstrated the therapeutic effects of NSA, a pharmacological MLKL inhibitor, in an acute MPTP mouse model of PD. NSA reversed the loss of dopaminergic cells in the SN and restored impaired neurotransmission to the striatum. NSA also inhibited microglial/astrocyte activation and the expression of proinflammatory markers in the SN of MPTP mice. Furthermore, it reduced oxidative stress by activating the Nrf2 antioxidant signaling pathway. Finally, we demonstrated that NSA inhibits p-MLKL expression in dopaminergic neurons and activated microglia, suggesting the involvement of MLKL in neuronal cell death and neuroinflammation. The effects of the NSA are summarized in Fig. 5.

Previous *in vivo* experiments in MLKL knockout mice have shown that MLKL mediates neuroinflammation. Lin *et al*. (2020) observed that deletion of MLKL decreased the elevation of inflammatory cytokines in MPTP-treated mice, indicating that MLKL modulates neuroinflammation (Lin *et al*., 2020). Geng *et al*. (2023) found that MLKL deficiency alleviates neuroinflammation by suppressing microglial activation in an α-synuclein transgenic mouse model of PD (Geng *et al*., 2023). Multiple studies have shown that MLKL modulates the activation of the NLRP3 inflammasome. Activation of MLKL in monocytes and bone marrow-derived macrophages (BMDMs) leads to the stimulation of the NLRP3 inflammasome and promotes caspase-1-dependent processing and secretion of IL-1β in a cell-intrinsic manner (Kang *et al*., 2015; Conos *et al*., 2017; Martens *et al*., 2021). Consistent with these findings, our study showed that pharmacological inhibition of MLKL using NSA reduced the expression of proinflammatory markers by regulating microglial and astrocyte activation in MPTP-treated mice. These results further highlight the role of MLKL as a key mediator of neuroinflammation and suggest the therapeutic potential of NSA in neuroinflammatory disorders, such as PD.

Previous studies have reported that ROS play critical

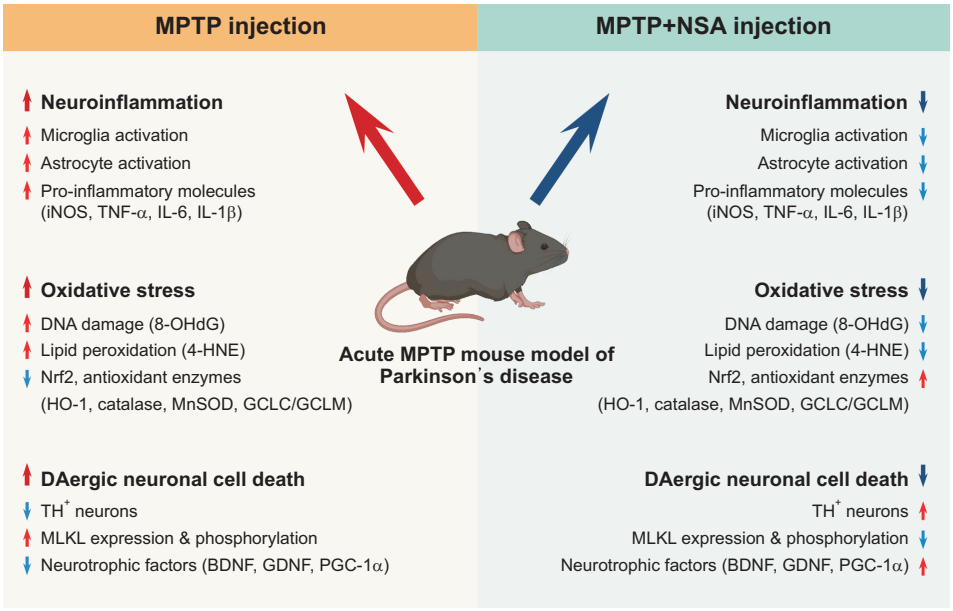

Fig. 5. Schematic representation of the effects of NSA in the brains of MPTP-injected mice. NSA attenuates neuroinflammation by reducing the activation of microglia and astrocytes and downregulating the expression of proinflammatory molecules. It also mitigated oxidative stress by enhancing Nrf2-mediated antioxidant enzyme expression, thereby decreasing markers such as 8-OHdG and 4-HNE. Further, NSA protected against dopaminergic neuronal cell death by suppressing MLKL activity and promoting the restoration of neurotrophic factors. MPTP, 1-methyl-4-phenyl-1,2,3,6-tetrahydropyridine; iNOS, inducible nitric oxide synthase; TNF-α, tumor necrosis factor-α; IL-1β, interleukin-1β; 8-OHdG, 8-hydroxy-2'-deoxyguanosine; 4-HNE, 4-hydroxynonenal; Nrf2, nuclear factor erythroid 2-related factor 2; HO-1, hemeoxygenase-1; MnSOD, manganese superoxide dismutase; GCLC, γ-glutamyl cysteine ligase-catalytic subunit; GCLM, γ-glutamyl cysteine ligase-modulator subunit; TH, tyrosine hydroxylase; MLKL, mixed lineage kinase domain-like protein; BDNF, brain-derived neurotrophic factor; GDNF, glial cell-derived neurotrophic factor; PGC-1α, peroxisome proliferator-activated receptor-gamma coactivator-1 alpha.

roles in necroptotic signaling and inflammation. ROS induces RIPK1 phosphorylation, RIPK1/3 necrosome assembly, and MLKL activation, resulting in necroptotic cell death (Schenk and Fulda, 2015; Zhang *et al*., 2017; Xue *et al*., 2020). Conversely, several studies have reported that MLKL mediates ROS production during necroptosis (Schenk and Fulda, 2015; Yang *et al*., 2018; Xue *et al*., 2020). MLKL induces ROS production and late-phase JNK activation in TSZ (TNF-α, Smac mimetic, and z-VAD)-treated HT-29 cells (Zhao *et al*., 2012; Chu, 2013). Additionally, ROS function upstream and downstream of MLKL activation in TNF/BV6-treated necroptotic cells, thereby creating a positive feedback loop between MLKL and ROS production (Schenk and Fulda, 2015). In the present study, we observed that NSA reduced the levels of oxidative stress markers, including 4-HNE and 8-OHdG in the SN of MPTP-treated mice. Additionally, NSA inhibited MLKL phosphorylation in necroptotic neurons and microglia, suggesting a potential positive feedback loop between ROS production and MLKL-driven necroptosis.

Regarding the antioxidant mechanism of NSA, this study revealed that NSA enhances the expression of Nrf2 and its downstream antioxidant enzymes, including HO-1, catalase, MnSOD, and GCLC/GCLM. These findings are consistent with those of previous studies showing that NSA alleviates neurological deficits in spinal cord injury by increasing glutathione and superoxide dismutase levels and reducing ROS and malonyldialdehyde (Jiao *et al*., 2020). Additionally, NSA has demonstrated protective effects against doxorubicin-induced cardiotoxicity by restoring antioxidant enzymes such as HO-1 and glutathione peroxidase-4 (Abbas *et al*., 2023). Given that the aforementioned antioxidant enzymes (HO-1, catalase, SOD, GPX-4, and GCLC/GCLM) are regulated by Nrf2, NSA-mediated activation of the Nrf2 antioxidant pathway may be pivotal in reducing ROS levels and inhibiting the necroptotic process in our study and other disease models.

In conclusion, this study revealed that NSA exerts neuroprotective effects by mitigating oxidative stress and neuroinflammation in an MPTP-induced PD mouse model. Therefore, NSA has emerged as a promising candidate for therapeutic intervention in PD, which is characterized by necroptosis and neuroinflammatory processes.

CONFLICT OF INTEREST

The authors declare no competing interests.

ACKNOWLEDGMENTS

This research was supported by a National Research Foundation of Korea (NRF) grant funded by the Korean government (MSIT) (Grant No. NRF-2020R1A5A2019210).

REFERENCES

Abbas, S. F., Abdulkadim, H.andHadi, N. R. (2023) Assessing the cardioprotective effect of necrosulfonamide in doxorubicin-induced cardiotoxicity in mice. *J. Med. Life* **16**,1468-1473.

Antonini, A., Emmi, A. and Campagnolo, M. (2023) Beyond the dopaminergic system: lessons learned from levodopa resistant symptoms in Parkinson's disease. *Mov. Disord. Clin. Pract.* **10**, S50-S55.

Caccamo, A., Branca, C., Piras, I. S., Ferreira, E., Huentelman, M. J., Liang,W. S., Readhead, B., Dudley, J. T., Spangenberg, E. E., Green, K. N., Belfiore, R., Winslow, W. and Oddo, S. (2017) Necroptosis activation in Alzheimer's disease. *Nat. Neurosci.* **20**, 1236-1246.

Calabresi, P., Mechelli, A., Natale, G., Volpicelli-Daley, L., Di Lazzaro, G. and Ghiglieri, V. (2023) Alpha-synuclein in Parkinson's disease and other synucleinopathies: from overt neurodegeneration back to early synaptic dysfunction. *Cell Death Dis.* **14**, 176.

Chang, K. H. and Chen, C. M. (2020) The role of oxidative stress in Parkinson's disease. *Antioxidants (Basel)* **9**, 597.

Chu, W. M. (2013) Tumor necrosis factor. *Cancer Lett.* **328**, 222-225.

Conos, S. A., Chen, K. W., De Nardo, D., Hara, H., Whitehead, L., Núñez, G., Masters, S. L., Murphy, J. M., Schroder, K., Vaux, D. L., Lawlor, K. E., Lindqvist, L. M. and Vince, J. E. (2017) Active MLKL triggers the NLRP3 inflammasome in a cell-intrinsic manner. *Proc. Natl. Acad. Sci. U. S. A.* **114**, E961-E969.

Fu, Q., Zhang, Y. B., Shi, C. X., Jiang, M., Lu, K., Fu, Z. H., Ruan, J. P., Wu, J. and Gu, X. P. (2024) GSDMD/Drp1 signaling pathway mediates hippocampal synaptic damage and neural oscillation abnormalities in a mouse model of sepsis-associated encephalopathy. *J. Neuroinflammation* **21**, 96.

Furgiuele, A., Pereira, F. C., Martini, S., Marino, F. and Cosentino, M. (2023) Dopaminergic regulation of inflammation and immunity in Parkinson's disease: friend or foe? *Clin. Transl. Immunology* **12**, e1469.

Geng, L., Gao, W., Saiyin, H., Li, Y., Zeng, Y., Zhang, Z., Li, X., Liu, Z., Gao, Q., An, P., Jiang, N., Yu, X., Chen, X., Li, S., Chen, L., Lu, B., Li, A., Chen, G., Shen, Y., Zhang, H., Tian, M., Zhang, Z. and Li, J. (2023) MLKL deficiency alleviates neuroinflammation and motor deficits in the alpha-synuclein transgenic mouse model of Parkinson's disease. *Mol. Neurodegener.* **18**, 94.

Henrich, M. T., Oertel, W. H., Surmeier, D. J. and Geibl, F. F. (2023) Mitochondrial dysfunction in Parkinson's disease - a key disease hallmark with therapeutic potential. *Mol. Neurodegener.* **18**, 83.

Ito, Y., Ofengeim, D., Najafov, A., Das, S., Saberi, S., Li, Y., Hitomi, J., Zhu, H., Chen, H., Mayo, L., Geng, J., Amin, P., DeWitt, J. P., Mookhtiar, A. K., Florez, M., Ouchida, A. T., Fan, J. B., Pasparakis, M., Kelliher, M. A., Ravits, J. and Yuan, J. (2016) RIPK1 mediates axonal degeneration by promoting inflammation and necroptosis in ALS. *Science* **353**, 603-608.

Jackson-Lewis, V. and Przedborski, S. (2007) Protocol for the MPTP mouse model of Parkinson's disease. *Nat. Protoc.* **2**, 141-151.

Jiao, J., Wang, Y., Ren, P., Sun, S. and Wu, M. (2020) Necrosulfonamide ameliorates neurological impairment in spinal cord injury by improving antioxidative capacity. *Front. Pharmacol.* **10**, 1538.

Kang, S.,Fernandes-Alnemri, T., Rogers, C., Mayes, L., Wang, Y., Dillon, C., Roback, L., Kaiser, W., Oberst, A., Sagara, J., Fitzgerald, K. A., Green, D. R., Zhang, J., Mocarski, E. S. and Alnemri, E. S. (2015) Caspase-8 scaffolding function and MLKL regulate NLRP3 inflammasome activation downstream of TLR3. *Nat. Commun.* **6**, 7515.

Kearney, C. J. and Martin, S. J. (2017) An inflammatory perspective on necroptosis. *Mol. Cell* **65**, 965-973.

Leem, Y. H., Kim, D. Y., Park, J. E. and Kim, H. S. (2023) Necrosulfonamide exerts neuroprotective effect by inhibiting necroptosis, neuroinflammation, and alpha-synuclein oligomerization in a subacute MPTP mouse model of Parkinson's disease. *Sci. Rep.* **13**, 8783.

Lin, Q. S., Chen, P., Wang, W. X., Lin, C. C., Zhou, Y., Yu, L. H., Lin, Y. X., Xu, Y. F. and Kang, D. Z. (2020) RIP1/RIP3/MLKL mediates dopaminergic neuron necroptosis in a mouse model of Parkinson disease. *Lab. Invest.* **100**, 503-511.

Liu, S., Liu, H., Johnston, A., Hanna-Addams, S., Reynoso, E., Xiang, Y. and Wang Z. (2017) MLKL forms disulfide bond-dependent amyloid-like polymers to induce necroptosis. *Proc. Natl. Acad. Sci. U. S. A.* **114**, E7450-E7459.

Martens, S., Bridelance, J., Roelandt, R., Vandenabeele, P. and Takahashi, N. (2021) MLKL in cancer: more than a necroptosis regulator. *Cell Death Differ.* **28**, 1757-1772.

Molnár, T., Mázló, A., Tslaf, V., Szöllősi, A. G., Emri, G. and Koncz, G. (2019) Current translational potential and underlying molecular

mechanisms of necroptosis. *Cell Death Dis.* **10**, 860.
Motawi, T. M. K., Abdel-Nasser, Z. M. and Shahin, N. N. (2020) Ameliorative effect of necrosulfonamide in a rat model of Alzheimer's disease: targeting mixed lineage kinase domain-like protein-mediated necroptosis. *ACS Chem. Neurosci.* **11**, 3386-3397.
Ofengeim, D., Ito, Y., Najafov, A., Zhang, Y., Shan, B., DeWitt, J. P., Ye, J., Zhang, X., Chang, A., Vakifahmetoglu-Norberg, H., Geng, J., Py, B., Zhou, W., Amin, P., Berlink Lima, J., Qi, C., Yu, Q., Trapp, B. and Yuan, J. (2015) Activation of necroptosis in multiple sclerosis. *Cell Rep.* **10**, 1836-1849.
Ozgen, B., Senol, S. P., Yilmaz, D. E., Temiz-Resitoglu, M., Bahceli, O. and Tunctan, B. (2023) Pyroptosis and necroptosis inhibitor necrosulfonamide ameliorates lipopolysaccharide-induced inflammatory hyperalgesia in mice. *Pharmacia* **70**, 1345-1354.
Poewe, W., Seppi, K., Tanner, C. M., Halliday, G. M., Brundin, P., Volkmann, J., Schrag, A. E. and Lang, A. E. (2017) Parkinson disease. *Nat. Rev. Dis. Primers* **3**, 17013.
Rai, S. N. and Singh, P. (2020) Advancement in the modelling and therapeutics of Parkinson's disease. *J. Chem. Neuroanat.* **104**, 101752.
Rathkey, J. K., Zhao, J., Liu, Z., Chen, Y., Yang, J., Kondolf, H. C., Benson, B. L., Chirieleison, S. M., Huang, A. Y., Dubyak, G. R., Xiao, T. S., Li, X. and Abbott, D. W. (2018) Chemical disruption of the pyroptotic pore-forming protein gasdermin D inhibits inflammatory cell death and sepsis. *Sci. Immunol.* **3**, eaat2738.
Schenk, B. and Fulda, S. (2015) Reactive oxygen species regulate Smac mimetic/TNFα-induced necroptotic signaling and cell death. *Oncogene* **34**, 5796-5806.
Stocchi, F., Bravi, D., Emmi, A. and Antonini, A. (2024) Parkinson disease therapy: current strategies and future research priorities. *Nat. Rev. Neurol.* **20**, 695-707.
Tang, Y. and Zhuang, C. (2024) Design, synthesis and anti-necroptosis activity of fused heterocyclic MLKL inhibitors. *Bioorg. Med. Chem.* **102**, 117659.
Taylor, J. M., Main, B. S. and Crack, P. J. (2013) Neuroinflammation and oxidative stress: co-conspirators in the pathology of Parkinson's disease. *Neurochem. Int.* **62**, 803-819.
Xue, C., Gu, X., Li, G., Bao, Z. and Li, L. (2020) Mitochondrial mechanisms of necroptosis in liver diseases. *Int. J. Mol. Sci.* **22**, 66.
Yang, Z., Wang, Y., Zhang, Y., He, X., Zhong, C. Q., Ni, H., Chen, X., Liang, Y., Wu, J., Zhao, S., Zhou, D. and Han, J. (2018) RIP3 targets pyruvate dehydrogenase complex to increase aerobic respiration in TNF-induced necroptosis. *Nat. Cell Biol.* **20**, 186-197.
Ye, H., Robak, L. A., Yu, M., Cykowski, M. and Shulman, J. M. (2023) Genetics and pathogenesis of Parkinson's syndrome. *Annu. Rev. Pathol.* **18**, 95-121.
Zhang, X., Zhang, Y., Wang, F., Liu, Y., Yong, V. W. and Xue, M. (2022) Necrosulfonamide alleviates acute brain injury of intracerebral hemorrhage via inhibiting inflammation and necroptosis. *Front. Mol. Neurosci.* **15**, 916249.
Zhang, Y., Su, S. S., Zhao, S., Yang, Z., Zhong, C. Q., Chen, X., Cai, Q., Yang, Z. H., Huang, D., Wu, R. and Han, J. (2017) RIP1 autophosphorylation is promoted by mitochondrial ROS and is essential for RIP3 recruitment into necrosome. *Nat. Commun.* **8**, 14329.
Zhao, J., Jitkaew, S., Cai, Z., Choksi, S., Li, Q., Luo, J. and Liu, Z. G. (2012) Mixed lineage kinase domain-like is a key receptor interacting protein 3 downstream component of TNF-induced necrosis. *Proc. Natl. Acad. Sci. U. S. A.* **109**, 5322-5327.
Zhou, X.Y., Lin, B., Chen, W., Cao, R. Q., Guo, Y., Said, A., Khan, T., Zhang, H. L. and Zhu, Y. M. (2023) The brain protection of MLKL inhibitor necrosulfonamide against focal ischemia/reperfusion injury associating with blocking the nucleus and nuclear envelope translocation of MLKL and RIP3K. *Front. Pharmacol.* **14**, 1157054.